Small-Angle Neutron Scattering Study on End-Linked Poly(tetrahydrofuran) Networks

Mitsuhiro Shibayama,* Hiroshi Takahashi, and Shunji Nomura

Department of Polymer Science and Engineering, Kyoto Institute of Technology, Matsugasaki, Sakyo-ku, Kyoto 606, Japan

Received March 7, 1995; Revised Manuscript Received June 27, 1995[⊗]

ABSTRACT: The relationship holding between the degree of polymerization between cross-links, N, the volume fraction at swelling equilibrium, ϕ, and the correlation length, ξ, for end-linked poly(tetrahydrofuran) (PTHF) networks having a fairly narrow molecular weight distribution was studied by swelling and small-angle neutron scattering (SANS) experiments. A scaling rule, $\phi \sim N^{-0.74}$, was obtained for the PTHF networks swollen in toluene. This result agrees with the scaling prediction, $\phi \sim N_{blob}^{-4/5}$, for semidilute polymer solutions, where N_{blob} is the degree of polymerization for a subchain in a blob. SANS spectra from PTHF networks swollen in deuterated toluene indicated the presence of two types of concentration fluctuations, i.e., solution-like fluctuations characterized by the correlation length, ξ, and solid-like fluctuations due to screening breakdown of cross-links. ξ was found to be given by $\xi \sim N^{0.59}$. This led to $\xi \sim \phi^{-0.79}$, which was also in good agreement with the scaling prediction ($\xi \sim \phi^{-3/4}$).

Introduction

Properties of swollen polymer networks have been extensively studied by mechanical and thermodynamic experiments.[1-3] It is well known that the volume fraction of networks at swelling equilibrium is well predicted by Flory–Rehner theory[1,2] and some other theories, such as the phantom network theory.[4] However, the structure–properties relationship of polymer networks has not been well elucidated mainly due to spatial inhomogeneities introduced by cross-links. Spatial inhomogeneities have been investigated by scattering methods, namely, light scattering, small-angle X-ray (SAXS) and neutron scattering (SANS), many of which are summarized in relevant review papers by Candau et al.[5] and Bastide.[6] An interesting comparison of the structure factors among statistically cross-linked gel, end-linked gel, and the corresponding semidilute polymer solutions was made by Bastide et al.[7] The intensity upturn at low scattering angle was highest for the statistically cross-linked gel, followed by the end-linked gel, and no noticeable intensity increase was observed for the polymer solutions. The effect of cross-links can be discussed based on the work by Mendes et al.[8] They compared small-angle neutron scattering intensity functions of polystyrene networks in deuterated toluene before and after cross-linking and found no significant difference in the intensity functions. However, by swelling the gel, a remarkable increase in the scattered intensity in the low scattering angle region was observed. This phenomenon was well explained by a blob percolation model.[9] Another interesting experiment was conducted by Mendes et al.[10] They examined the structure factor of end-linked polymer gels having different degrees of swelling. The scattered intensity at low scattering angle became stronger with increasing degree of swelling. However, since types of inhomogeneities depend greatly on the manner and history of network preparation, the nature of cross-linking inhomogeneities has not been well elucidated.

Polymer networks comprising telechelic poly(tetrahydrofuran) (PTHF) followed by end-coupling with a multifunctional coupling agent are one of the most suitable systems for studying network inhomogeneities because of the availability of deuterated tetrahydrofuran monomer and the capability of carrying out a living cationic polymerization which leads to a fairly monodisperse prepolymer. Hanyu and Stein studied cross-linking inhomogeneities on bimodal networks consisting of long and short chains.[11] We studied the crystallization kinetics of end-linked PTHF networks.[12,13] It was found that the PTHF network forms spherulitic superstructures although both chain ends are cross-linked and the crystallization kinetics is greatly dependent on the prepolymer molecular weight.[13]

In this paper, we employ a series of unimodal model polymer networks having a narrow molecular weight distribution and investigate the relationship between the polymer concentration, the molecular weight between cross-links, and the structure factors on the basis of results of small-angle neutron scattering and swelling experiments.

Experimental Section

1. Samples. A series of telechelic poly(tetrahydrofuran) (PTHF) prepolymers having allyl groups at both ends were synthesized by living cationic polymerization. The details of sample preparation are described elsewhere.[12] Table 1 shows the sample characteristics of the prepolymers. The number-average molecular weight, M_n, was determined by vapor pressure osmometry (VPO, Knauer). The numbers in the sample code indicate M_n. The third column in Table 1 shows the number of THF monomers per prepolymer (i.e., the degree of polymerization), N, calculated by taking account of the molecular weight of the end groups. The polydispersity index, the ratio of the weight- and number-average molecular weights, M_w/M_n, was evaluated with a Trirotar II GPC (Jasco Co., Ltd., Japan). The functionality of the allyl end groups were evaluated with a 300 MHz QE-300 NMR spectrometer (General Electric). Preparation of unimodal model networks was conducted by using these prepolymers. A small amount of prepolymer was transferred into a stainless steel mold and a network film was prepared with a four-functional cross-link reagent, pentaerythritol tetrakis(3-mercaptopropionate). After preparation of networks, sol fraction, ranging from 5 to 30 wt % depending on M_n, was extracted by immersing the network in toluene repeatedly.

* To whom correspondence should be addressed.

[⊗] Abstract published in *Advance ACS Abstracts,* September 1, 1995.

0024-9297/95/2228-6860$09.00/0

Table 1. Characterization of Prepolymers and Sol Fraction of As-Prepared Networks

sample code	prepolymer				sol fraction
	$M_n \times 10^{-3}$ [a]	N	M_w/M_n [b]	functionality [c]	
U025	2.54	34.1	1.15	1.85	0.05
U044	4.36	59.3	1.17	2.02	0.10
U052	5.19	70.8	1.17	1.94	0.09
U079	7.91	109	1.18	1.94	0.19
U102	10.2	140	1.20	2.09	0.30

[a] By VPO. [b] By GPC. [c] By ^{1}H NMR.

2. Swelling Experiment. Network films cut to a disk form were swollen in toluene or in cyclohexane at 25 °C. The degree of swelling was determined by measuring the diameters of the film before and after swelling.

3. SANS. Small-angle neutron scattering experiments were carried out at the research reactor SANS-U, Institute of Solid State Physics, The University of Tokyo, located at the Japan Atomic Energy Research Institute, Tokai, Japan. Cold neutrons having the wavelength of $\lambda = 7$ Å were used as the incident beam. Each network sample at swelling equilibrium with deuterated toluene was sealed in a brass cell having quartz windows, of which the optical path length was about 2 mm. Then the sample was irradiated by the neutron beam for 30 min and the scattered intensity was counted with an area detector. The observed scattered intensity was corrected for cell scattering, transmission, solvent scattering, and fast neutrons and then rescaled to the absolute intensity with a secondary standard sample of a Lupolen.[14]

Results and Discussion

1. Equilibrium Swelling. The volume fraction of the network, ϕ, at swelling equilibrium was estimated from the linear swelling ratio, d/d_0, by

$$\phi = (d_0/d)^3 \tag{1}$$

where d_0 and d are the characteristic sizes of the network film, namely, the diameters before and after swelling, respectively.

First of all, we examined the molecular weight between cross-links by using the Flory–Rehner equation.[1,2] The equation is given by

$$\ln(1-\phi) + \phi + \chi\phi^2 = -\left(\frac{V_1}{\bar{v}M_c}\right)\left(\phi^{1/3} - \frac{\phi}{2}\right) \tag{2}$$

for affine networks and

$$\ln(1-\phi) + \phi + \chi\phi^2 = -\frac{1}{2}\left(\frac{V_1}{\bar{v}M_c}\right)\phi^{1/3} \tag{3}$$

for phantom networks,[4,15] where V_1 is the molar volume of the solvent, χ is the Flory interaction parameter, and $\bar{v}$ is the specific volume of the polymer (≈1.02 cm^3/g). The χ parameter for PTHF in cyclohexane is reported by Shiomi et al.[16] as

$$\chi = 0.447 + 0.235\phi \quad \text{(at 25 °C)} \tag{4}$$

Figure 1 shows the ratio of the molecular weight between cross-links, M_c, estimated with eqs 2 and 3 to the prepolymer molecular weight, M_n, estimated by VPO, $(M_n)_{VPO}$. As shown in the figure, good agreement between M_c and $(M_n)_{VPO}$ ($\equiv M_n$) was obtained except for U102. Furthermore, the affine network model seems to be more appropriate than the phantom network model to describe the system. The deviation for U102 is ascribed to a low efficiency of cross-linking reaction as indicated in Table 1 (sol fraction of about 30 wt %).

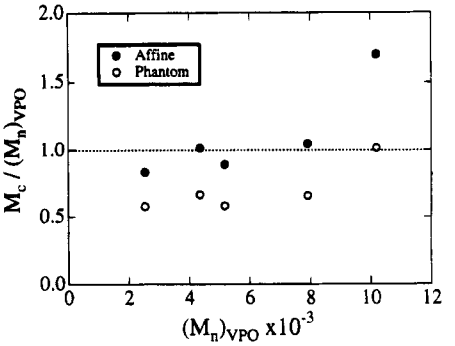

Figure 1. Comparison of the molecular weights between cross-links measured by swelling equilibrium, M_c, and by VPO, $(M_n)_{VPO}$.

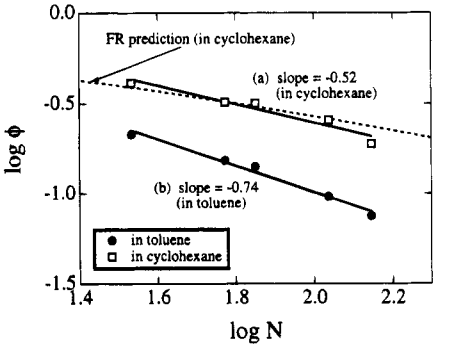

Figure 2. Polymer volume fraction, ϕ, at swelling equilibrium in (a) cyclohexane and (b) toluene as a function of the degree of polymerization between cross-links, N. The dashed line indicates the predicted ϕ variation in cyclohexane on the basis of the Flory–Rehner equation (eq 2).

Since it is assumed that the functionality of cross-linker, f, is 4 in eqs 2 and 3, a decrease of f leads to an overestimation of M_c. The efficiency of the coupling reaction is extensively discussed in a forthcoming paper.[17]

Figure 2 shows the variations of ϕ (the volume fraction of the network at swelling equilibrium) in (a) cyclohexane and (b) toluene as a function of N. The dashed line indicates the ϕ variation predicted by the Flory–Rehner equation (eq 2) for cyclohexane solution. As seen in the figure, ϕ's are decreasing functions of N both for cyclohexane and toluene solutions and the data points roughly fall on straight lines, given by

$$\phi \sim N^{-0.52} \quad \text{for a network in cyclohexane} \tag{5a}$$

$$\phi \sim N^{-0.74} \quad \text{for a network in toluene} \tag{5b}$$

The exponents clearly indicate the difference in the solvnt nature, i.e., near a Θ solvent (cyclohexane) and a rather good solvent (toluene). Note that the values of ϕ for the network in cyclohexane are more than twice as large as that for the network in toluene. These exponents are close to the values of the scaling prediction for a semidilute polymer solution and/or polymer networks in a swelling equilibrium in a Θ solvent ($-1/2$) and in a good solvent ($-4/5$).[18] Therefore, it seems that the network consists of space-filled blobs of which the segment number is N. In the following sections, we discuss only the case of swollen networks in toluene so as to clarify the relationship between the molecular parameter (N), the thermodynamic properties (ϕ), and the structure parameters in the good solvent regime.

2. SANS. As was discussed in the Introduction, small-angle scattering from a swollen network consists

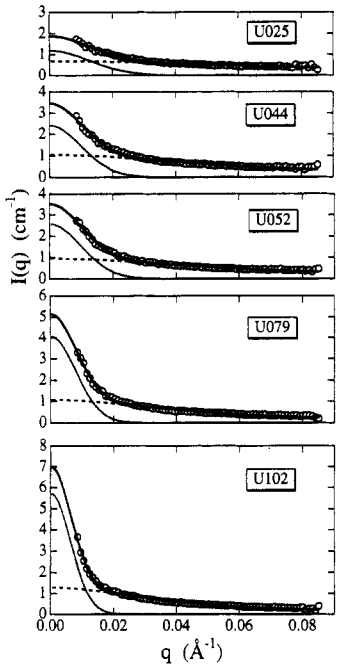

Figure 3. SANS intensity profiles for the unimodal polymer networks at swelling equilibrium. Open circles, dotted curves, and dashed curves denote observed scattered intensity profiles, the Gauss component and the Lorentz component, respectively. The solid curves indicate reconstructed intensity profiles.

of solution-like and solid-like concentration fluctuations. The former is simply given by a Lorentz (Ornstein–Zernike) type function.[18] On the other hand, there is no deterministic function to represent the solid-like fluctuations since these are frozen-in fluctuations, dependent on the manner of network preparation, dispersity of the network, and so on. Therefore, we simply employ a combination of Gauss and Lorentz functions, originally proposed by Geissler and co-workers,[19–23]

$$I(q) = I_G(0) \exp\left[-\frac{\Xi^2 q^2}{3}\right] + \frac{I_L(0)}{1+\xi^2 q^2} \qquad (6)$$

where q is the magnitude of the scattering vector and $I_G(0)$ and Ξ represent the zero-q intensity and the characteristic mean size of the static (frozen) inhomogeneity (assemblies of monomer-rich "domains"), respectively. The Gaussian term can be read as a Guinier function of which Ξ is the radius of gyration of the domains. The second term on the right-hand side of eq 6 represents liquid-like (dynamic) fluctuations, and $I_L(0)$ and ξ are the zero-q intensity and the correlation length, respectively. Figure 3 shows a series of SANS intensity profiles. The open circles indicate the observed scattered intensity, and the dotted and dashed curves denote the Gauss and Lorentz components, respectively. The curve fitting was conducted in the range of $0.0085 \le q \le 0.081$ Å^{-1}. It should be noted here that the decomposition method (eq 6) includes some ambiguities since the shape of the solid-like contribution is not well established. We will take into account this point in the following discussion.

Figure 4 shows the estimated structure parameters Ξ and ξ as a function of N. Both Ξ and ξ increase with N, indicating increases in the scale of inhomogeneities. The values of Ξ are about 7–8 times larger than those of ξ. Figure 5 shows the variation of $I_G(0)$ and $I_L(0)$ with N. The increase of $I_L(0)$ with N seems to be reasonable because the scattering body characterized by ξ is

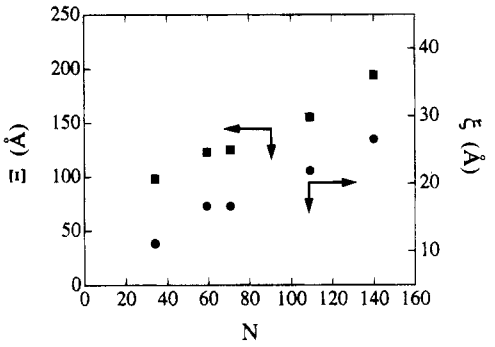

Figure 4. N dependencies of the structure parameters ξ and Ξ.

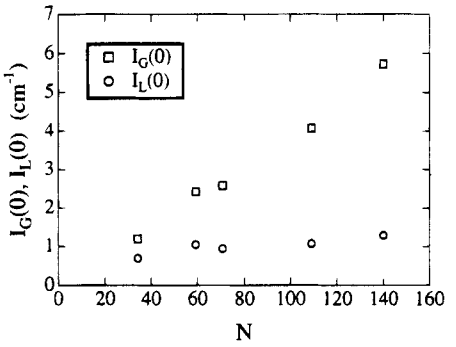

Figure 5. N dependencies of the structure parameters $I_G(0)$ and $I_L(0)$.

increasing with N. However, the increase of $I_G(0)$ with N was rather suprising since we expected a decrease of the static inhomogeneities by increasing N. This problem will be discussed later.

3. Scaling Rules for Solution-like Concentration Fluctuations. According to the so-called C^* theorem,[18] the correlation length of a network at swelling equilibrium is the same as that for the corresponding polymer solution having the same concentration. This concentration, where chains start to overlap (or subchains in a swollen network), is given by

$$C^* = \frac{\phi^*}{a^3} \cong \frac{N}{R_F^3} \sim N^{-4/5} \qquad (7)$$

where C^* and a are the monomer number concentration of the polymer and the segment length, respectively. R_F is the Flory radius of the polymer chain. In the case of polymer networks at swelling equilibrium, N and ϕ are the degree of polymerization between cross-links and polymer volume fraction, respectively. Thus,

$$\phi \cong a^3 \frac{N}{\xi^3} \sim N^{-4/5} \qquad (8)$$

On the other hand, ξ is simply given by

$$\xi \cong aN^{3/5} \qquad (9)$$

for blobs in an athermal solvent. By substituting eq 8 into eq 9, one gets

$$\xi \cong a\phi^{-3/4} \qquad (10)$$

Equations 8–10 are the relationship among the polymer mass (N), swelling power (characterized by ϕ), and the characteristic structure (ξ) expected for a network at swelling equilibrium. The zero-angle scattered intensity, $I_L(0)$, on the other hand, is related to the osmotic

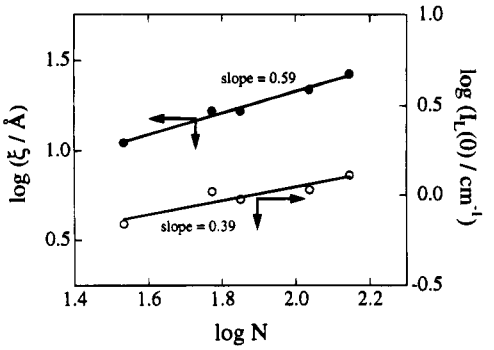

Figure 6. Scaling rules for ξ and $I_L(0)$ with N.

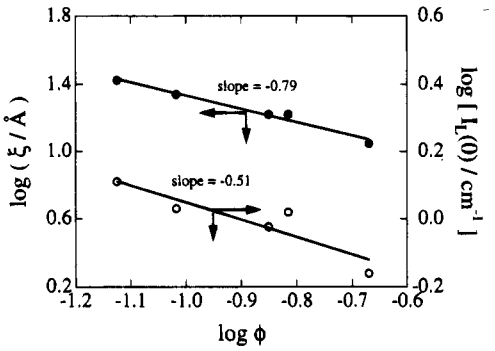

Figure 7. Scaling rules for ξ and $I_L(0)$ with ϕ.

bulk modulus, $K = \phi(\partial\Pi/\partial\phi)_T$. In the case of semidilute polymer solutions, the following equation is given,

$$I_L(0) \sim \frac{\phi^2}{K} = \frac{\phi}{(\partial\Pi/\partial\phi)_T} \sim \phi^{-1/4}$$

(for a semidilute solution) (11a)

where Π is the osmotic pressure and T is the absolute temperature. Thus a simple scaling relation is obtained between $I_L(0)$ and ϕ. However, in the case of a polymer network in a solvent, eq 11a has to be modified to

$$I_L(0) \sim \frac{\phi^2}{K + 4\mu/3} \quad \text{(for a network in a solvent)} \tag{11b}$$

where μ is the shear modulus.[23] The term $(K + 4\mu/3)$ is called the osmotic longitudinal modulus. Since μ scales roughly as $\phi^{1/3}$, the ϕ dependence of $I_L(0)$ is expected to deviate from $I_L(0) \sim \phi^{-1/4}$ for a network in a solvent.[24]

Figure 6 shows double-logarithmic plots of ξ and $I_L(0)$ vs N. The data points roughly fall on a straight line both for ξ and for $I_L(0)$. From the slopes, scaling relationships can be drawn as follows:

$$\xi \sim N^{0.59} \tag{12}$$

$$I_L(0) \sim N^{0.39} \tag{13}$$

The observed exponent for ξ is in excellent agreement with the theoretical prediction of $^3/_5$ (eq 9).

Figure 7 shows the ϕ dependence of the structure parameters, ξ and $I_L(0)$. A linear regression analysis gives

$$\xi \sim \phi^{-0.79} \tag{14}$$

and

$$I_L(0) \sim \phi^{-0.51} \tag{15}$$

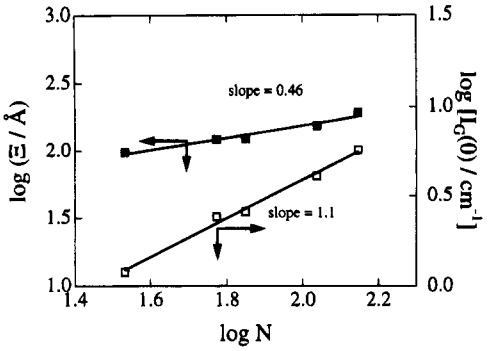

Figure 8. Scaling rules for Ξ and $I_G(0)$ with N.

The exponent -0.79 for ξ is again in good accordance with the theoretical prediction, $-^3/_4$, i.e., eq 10. However, the observed exponent for $I_L(0)$, -0.51, does not agree with the predicted one ($-^1/_4$). Although this discrepancy may be partially due to ambiguities related to the decomposition of the scattered intensity function (eq 6), the observed exponent indicates that the contribution of the shear modulus is noticeable. Therefore, it can be concluded that the solution-like fluctuations of the end-linked polymer network are well described by the scaling theory for polymer solutions in an athermal solvent at least for the characteristic size of the solution-like concentration fluctuations.

4. Scaling Rules for Solid-like Concentration Fluctuations. Now let us discuss the scaling relationship for the static fluctuations. Cross-linking inhomogeneities are observed as a result of screening breakdown of the initial random distribution of cross-link points.[9] Thus, it is assumed that cross-linking inhomogeneities can be represented by an assembly of monomer-rich "domains" where the domains do not interact with each other. In addition, the "domain" itself has a fractal dimension of D.[25] In this case, the mass of the "domain", m, can be related to its characteristic size, Ξ, as

$$\Xi \sim m^{1/D} \tag{16}$$

and the scattered intensity at $q = 0$ is given by[26]

$$I_G(0) \sim Cm \tag{17}$$

where C is the number concentration of the domain. Figure 8 shows double-logarithmic plots of Ξ and $I_G(0)$ vs N. This indicates that the total mass of the "domain", Cm, is related to N, and simple scaling relations can be extracted from this figure, which are

$$\Xi \sim N^{0.46} \tag{18}$$

$$I_G(0) \sim N^{1.1} \tag{19}$$

The origin of the strong correlation between m and N may be explained by one of the following two hypotheses: (1) The characteristic size of the solid-like fluctuations, Ξ, is directly related to N, or (2) this is given as a result of the N dependence of the volume fraction, ϕ, at swelling equilibrium. The latter means that Ξ is simply related to the degree of swelling; that is, the higher the swelling, the larger the Ξ.

Although further investigations are necessary in order to answer this question, the observed exponent for $I_G(0)$ with N is in good accordance with the prediction given by eq 17 if we reread Cm as N. The exponent for

Ξ may indicate that the characteristic mean size of the static fluctuations increases with $\Xi \sim N^{1/2}$(fractal) rather than $\Xi \sim N^{1/3}$ (densely packed three-dimensional objects). In other works, the characteristic mean size originating from a monomer-rich "domain" around cross-links has a mass fractal dimension of 2 according to the relation of eq 16. Hence, $D = 1/0.46 \approx 2$.

Concluding Remarks

Equilibrium swelling and small-angle neutron scattering experiments, which are independent of each other, were conducted on a series of end-linked poly(tetrahydrofuran) networks having a fairly narrow molecular weight distribution between cross-links. A well-correlated scaling relation holding between the mass, N, volume fraction, ϕ, and the correlation length, ξ, was observed for end-linked poly(tetrahydrofuran) networks having a narrow molecular weight distribution between cross-links. The scaling rules are $\phi \sim N^{-0.74}$, $\xi \sim \phi^{-0.79}$, and $\xi \sim N^{0.59}$, which are in good agreement with those from the scaling prediction. Structure parameters related to the static fluctuations were also evaluated as a function of N. The "domain" size, Ξ, and the zero-angle scattered intensity, $I_G(0)$, obey scaling rules with N, namely, $\Xi \sim N^{0.46}$ and $I_G(0) \sim N^{1.1}$. These relationships were successfully explained with a concept of fractal nature of this type of inhomogeneity.

Acknowledgment. This work is partially supported by a Grant-in-Aid, Ministry of Education, Science and Culture, Japan (Grant-in-Aid No. 06651053 to M.S.). The authors appreciate corrections and fruitful suggestions given by the reviewer. This work was performed with the approval of the Solid State Physics Laboratory, The University of Tokyo (Proposal No. 94-2) at the Japan Atomic Energy Research Institute, Tokai, Japan. The authors are grateful to Dr. M. Imai, Solid State Physics Laboratory, The University of Tokyo, for fruitful discussions.

References and Notes

(1) Flory, P. J.; Rehner, J., Jr. *J. Chem. Phys.* **1943**, *21*, 521.
(2) Flory, P. J. *Principles of Polymer Chemistry*; Cornell University Press: Ithaca, NY, 1953.
(3) Treloar, L. R. G. *The Physics of Rubber Elasticity*, 3rd ed.; Clarendon Press: Oxford, 1975.
(4) James, H. M.; Guth, E. *J. Chem. Phys.* **1947**, *15*, 669.
(5) Candau, S.; Bastide, J.; Delsanti, M. *Adv. Polym. Sci.* **1982**, *44*, 27.
(6) Bastide, J. In *Physical Properties of Gels*; Cotton-Addad, J. P., Ed.; Wiley: New York, 1995.
(7) Bastide, J.; Boue, F.; Buzier, M. *Springer Proc. Phys.* **1989**, *42*, 48.
(8) Mendes, E., Jr.; Lindner, P.; Muzier, M.; Boue, F.; Bastide, J. *Phys. Rev. Lett.* **1991**, *66*, 1595.
(9) Bastide, J.; Leibler, L. *Macromolecules* **1988**, *21*, 2647.
(10) Mendes, E.; Girard, B.; Picot, C.; Buzier, M.; Boue, F.; Bastide, J. *Macromolecules* **1993**, *26*, 6873.
(11) Hanyu, A.; Stein, R. S. *Makromol. Chem., Macromol. Symp.* **1991**, *45*, 189.
(12) Shibayama, M.; Takahashi, H.; Yamaguchi, H.; Sakurai, S.; Nomura, S. *Polymer* **1994**, *35*, 2944.
(13) Takahashi, H.; Shibayama, M.; Nomura, S. *Macromolecules* **1995**, *28*, 5547.
(14) Jinnai, H.; Schwahn, D.; Imai, M., unpublished results.
(15) Mark, J. E.; Erman, B. *Rubberlike Elasticity: A Molecular Primer*; Wiley: New York, 1988.
(16) Shiomi, T.; Kuroki, K.; Kobayashi, A.; Nikaido, H.; Yokoyama, M.; Tezuka, Y.; Imai, K. *Polymer* **1995**, *36*, 2443.
(17) Takahashi, H.; Shibayama, M.; Fujisawa, H.; Nomura, S. *Macromolecules*, submitted.
(18) de Gennes, P.-G. *Scaling Concepts in Polymer Physics*; Cornell University Press: Ithaca, NY, 1979.
(19) Hecht, A. M.; Duplessix, R.; Geissler, E. *Macromolecules* **1985**, *18*, 2167.
(20) Mallam, S.; Horkay, F.; Hecht, A.; Geissler, E. *Macromolecules* **1989**, *22*, 3356.
(21) Mallam, S.; Hecht, A. M.; Geissler, E. *J. Chem. Phys.* **1989**, *91*, 6447.
(22) Mallam, S.; Horkay, F.; Hecht, A. M.; Rennie, A. R.; Geissler, E. *Macromolecules* **1991**, *24*, 543.
(23) Horkay, F.; Hecht, A. M.; Mallam, S.; Geissler, E.; Rennie, A. R. *Macromolecules* **1991**, *24*, 2896.
(24) Geissler, G.; Horkay, F.; Hecht, A. M. *J. Chem. Phys.* **1994**, *100*, 8418.
(25) Stauffer, D. *Introduction to Percolation Theory*; Taylor & Francis: London, 1985.
(26) Martin, J. E.; Wilcoxon, J. P. *Phys. Rev. A* **1989**, *39*, 252.

MA9503017